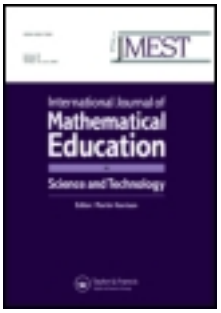

International Journal of Mathematical Education in Science and Technology

Publication details, including instructions for authors and subscription information:
http://www.tandfonline.com/loi/tmes20

The Gibbs' phenomenon for Fourier-Bessel series

Temple H. Fay [a] & P. Hendrik Kloppers [a]

[a] Technikon Pretoria and University of Southern Mississippi, Box 5045, Hattiesburg, MS39406-5045, USA Email: thfay@hotmail.com

Published online: 11 Nov 2010.

To cite this article: Temple H. Fay & P. Hendrik Kloppers (2003): The Gibbs' phenomenon for Fourier-Bessel series, International Journal of Mathematical Education in Science and Technology, 34:2, 199-217

To link to this article: http://dx.doi.org/10.1080/0020739021000053936

INT. J. MATH. EDUC. SCI. TECHNOL., 2003
VOL. 34, NO. 2, 199–217

Taylor & Francis
Taylor & Francis Group

The Gibbs' phenomenon for Fourier–Bessel series

TEMPLE H. FAY* and P. HENDRIK KLOPPERS
Technikon Pretoria and University of Southern Mississippi, Box 5045, Hattiesburg, MS39406-5045, USA
Email: thfay@hotmail.com

(*Received 18 December 2001*)

The paper investigates the Gibbs' phenomenon at a jump discontinuity for Fourier–Bessel series expansions. The unexpected thing is that the Gibbs' constant for Fourier–Bessel series appears to be the same as that for Fourier series expansions. In order to compute the coefficients for Fourier–Bessel functions efficiently, several integral formulas are derived and the Struve functions and their asymptotic expansions discussed, all of which significantly ease the computations. Three numerical examples are investigated. Findings suggest further investigations suitable for undergraduate research projects or small student group investigations.

1. Introduction

Beginning students in courses in partial differential equations, when employing the method of separation of variables, are introduced to Sturm–Liouville theory and the concepts of eigenfunctions and eigenvalues. Solving the heat equation and the wave equation over a circular domain leads to the eigenfunctions $\phi_n(x) = \mathcal{J}_0(\lambda_n x)$, where $\mathcal{J}_0(x)$ is a Bessel function of the first kind and eigenvalue λ_n is the nth positive zero of $\mathcal{J}_0(x)$. The property of the $\phi_n(x)$ being orthogonal with respect to the weight function $w(x) = x$, leads to eigenfunction expansions called *Fourier–Bessel series*. In many respects, such series behave similarly to Fourier series. The Gibbs' phenomenon for Fourier series has been investigated recently in this journal [1, 2] and it is natural to ask 'Is there a Gibbs' phenomenon for Fourier–Bessel series? And if so, what is the Gibbs' constant?'.

This article examines three examples, each having a jump discontinuity and the behaviour of truncated partial sums of Fourier–Bessel series representations is investigated numerically. In doing so, it was discovered, rather surprisingly, that the Gibbs' constant for the Fourier–Bessel series is the same (or appears to be the same) as the Fourier series Gibbs' constant for a jump discontinuity.

In particular, this investigation demonstrates:

- the usefulness of recursion relations and other formulas concerning the Bessel functions;
- Fourier–Bessel series, while convergent, are very slow to converge;

* The author to whom correspondence should be addressed.

International Journal of Mathematical Education in Science and Technology
ISSN 0020–739X print/ISSN 1464–5211 online © 2003 Taylor & Francis Ltd
http://www.tandf.co.uk/journals
DOI: 10.1080/0020739021000053936

- Fourier–Bessel series coefficients, defined by integral formulas, can be reduced to formulas involving less well-known functions called Struve functions;
- the efficacy of asymptotic expansions of the Struve functions for large arguments.

Some of the basic properties of Bessel functions and Struve functions, which are realized as particular solutions to non-homogeneous Bessel's equations, are briefly reviewed. The reader is also reminded of properties of the Fourier–Bessel series including remarks on convergence and calculation of the series coefficients. The behaviour of truncated sums of the Fourier–Bessel series is then investigated for a simple step function, a linear function, and a quadratic function, each defined over the interval $[0, 1]$ having a simple jump discontinuity at $x = 1/2$. A Gibbs' phenomenon is observed at this jump discontinuity and it is suggested, through numerical calculations, that the Gibbs' constant associated with this phenomenon is precisely the same as that which occurs for truncated sums of Fourier series. For the authors, this was quite unexpected and raises questions for further investigations, some of which are discussed in the final Conclusions section.

2. Bessel functions

Friedrich Wilhelm Bessel (1784–1846), in his study of planetary perturbations, developed the properties of solutions to what is now called *Bessel's equation of order* ν

$$x^2 \frac{\mathrm{d}^2 y}{\mathrm{d}x^2} + x \frac{\mathrm{d}y}{\mathrm{d}x} + (x^2 - \nu^2) y = 0 \tag{2.1}$$

where ν is a constant. This equation arises in many applied problems, and in particular in the solution to the heat equation in canonical units over the unit disc and to the vibrating circular membrane problem (the wave equation), when using the method of separation of variables; both of these problems are standard fare in a first course in partial differential equations. Two particular linearly independent solutions to this equation are called *Bessel functions of the first and second kind* and are denoted by $\mathcal{J}_\nu(x)$ and $Y_\nu(x)$ respectively. These functions are commonly discussed for $\nu = 0, 1$ in a beginning differential equations course when studying the method of Frobenius ($x = 0$ is a regular singular point of equation (2.1)). The computer algebra system *Mathematica* has function-calls **BesselJ[*ν*, x]** and **BesselY[*ν*, x]** that permit the user to effortlessly plot and compute with these functions (figure 1).

Because of the wide applicability of these functions, there is voluminous material written about them, and only a small part of this background material is highlighted. Although there are many series representations of these functions, only the *ascending* series is mentioned:

$$\mathcal{J}_\nu(x) = \left(\frac{x}{2}\right)^\nu \sum_{k=0}^{\infty} \frac{(-1)^k}{k!\Gamma(k + v + 1)} \left(\frac{x}{2}\right)^{2k} \tag{2.2}$$

where Γ is the Gamma function. For $\nu = 0$,

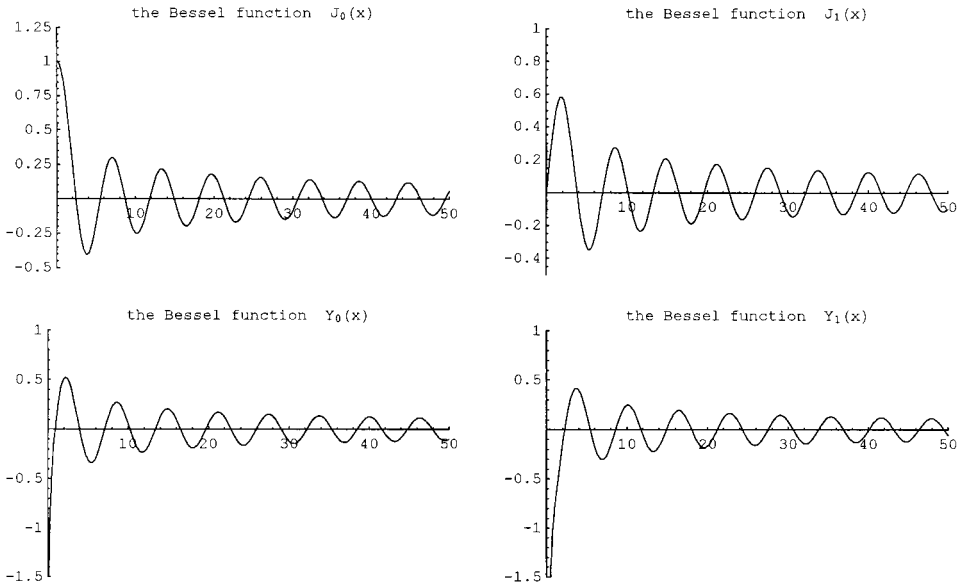

Figure 1. The Bessel functions $\mathcal{J}_\nu(x)$ and $Y_\nu(x)$ for $\nu = 0, 1$.

$$\mathcal{J}_0(x) = 1 + \sum_{k=1}^{\infty} \frac{(-1)^k x^{2k}}{2^{2k}(k!)^2} \tag{2.3}$$

and it follows that this series converges absolutely for all x. Note that $\mathcal{J}_0(x)$ is oscillatory with decreasing amplitude as $x \to \infty$, and has an infinite number of zeros which are labelled in increasing order as

$$\lambda_1, \lambda_2, \cdots, \lambda_n, \cdots$$

Values of these λs are easy to obtain using Newton's method or a *Mathematica* function-call named **BesselJZeros** which can generate them in a list.

There is a useful recurrence relation among the Bessel functions (see [3, p. 361])

$$\mathcal{J}_{v+1}(x) = \frac{2v}{x}\mathcal{J}_v(x) - \mathcal{J}_{v-1}(x) \tag{2.4}$$

In particular, with $v = 0$,

$$\mathcal{J}_1(x) = -\mathcal{J}_{-1}(x) \tag{2.5}$$

and with $v = 1$,

$$\mathcal{J}_2(x) = \frac{2}{x}\mathcal{J}_1(x) - \mathcal{J}_0(x) \tag{2.6}$$

It is also useful to observe the relations between derivatives [3, p. 361],

$$\frac{\mathrm{d}}{\mathrm{d}x}\mathcal{J}_\nu(x) = -\mathcal{J}_{v+1}(x) + \frac{\nu}{x}\mathcal{J}_\nu(x) \tag{2.7}$$

and

$$\frac{\mathrm{d}}{\mathrm{d}x}\mathcal{J}_\nu(x) = \frac{1}{2}\{\mathcal{J}_{v-1}(x) - \mathcal{J}_{\nu+1}(x)\} \tag{2.8}$$

In particular

$$\frac{\mathrm{d}}{\mathrm{d}x}\mathcal{J}_0(x) = -\mathcal{J}_1(x) \tag{2.9}$$

and

$$\frac{\mathrm{d}}{\mathrm{d}x}\mathcal{J}_1(x) = \frac{1}{2}\{\mathcal{J}_0(x) - \mathcal{J}_2(x)\} \tag{2.10}$$

From equations (2.6) and (2.10), it readily follows that

$$\frac{\mathrm{d}}{\mathrm{d}x}x\mathcal{J}_1(x) = x\mathcal{J}_0(x) \tag{2.11}$$

so that

$$\int x\mathcal{J}_0(x)\mathrm{d}x = x\mathcal{J}_1(x) \tag{2.12}$$

3. The Struve functions

The Struve functions, named after H. Struve[1] and denoted by $H_\nu(x)$, are used in science and engineering with applications in electromagnetic theory, electrodynamics and optics; in particular they are useful in designing microphone diaphragms [4]. According to Thompson [4, p. 435], 'The literature on these functions and on interrelations between them is quite sparse.' Some references are given in [4] and useful formulas are compiled in [3]. *Mathematica version 4* has a function-call **StruveH[*v*, x]** that permits using the Struve functions almost as effortlessly as the Bessel functions and trigonometric functions.

The Struve functions $H_\nu(x)$ are particular solutions to the non-homogeneous Bessel equation

$$x^2\frac{\mathrm{d}^2y}{\mathrm{d}x^2} + x\frac{\mathrm{d}y}{\mathrm{d}x} + (x^2 - \nu^2)y = \frac{4\left(\frac{x}{2}\right)^{\nu+1}}{\sqrt{\pi}\Gamma\left(\nu + \frac{1}{2}\right)} \tag{3.1}$$

where Γ is the Gamma function. That is, the general solution to equation (3.1) is of the form

$$y = c_1\mathcal{J}_\nu(x) + c_2\,Y_v(x) + H_\nu(x) \tag{3.2}$$

where c_1 and c_2 are arbitrary constants, $\mathcal{J}_\nu(x)$ and $Y_\nu(x)$ are the Bessel functions of the first and second kind of order ν, and $H_\nu(x)$ is the *Struve function of order* ν. For example, for $\nu = 0$ and 1 (figure 2), $H_0(x)$ and $H_1(x)$ are the respective particular solutions to

$$x^2\frac{\mathrm{d}^2y}{\mathrm{d}x^2} + x\frac{\mathrm{d}y}{\mathrm{d}x} + x^2y = \frac{2x}{\pi}$$

$$x^2\frac{d^2y}{\mathrm{d}x^2} + x\frac{\mathrm{d}y}{\mathrm{d}x} + (x^2 - 1^2)y = \frac{8x^2}{\pi}$$

[1] H. Struve, 1882, *Ann. Physik. Chemie*, **17**, 1008–1016.

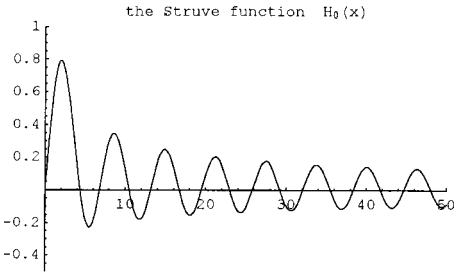

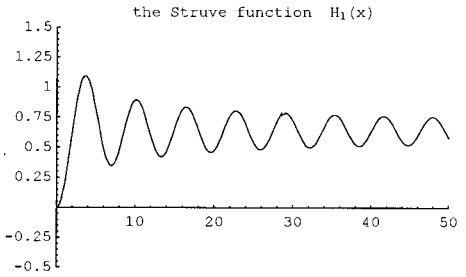

Figure 2. The Struve functions $H_\nu(x)$ for $\nu = 0, 1$.

The Struve function has a power series representation

$$H_v(x) = \left(\frac{x}{2}\right)^{\nu+1} \sum_{k=1}^{\infty} \frac{(-1)^k}{\Gamma\left(k+\frac{3}{2}\right)\Gamma\left(k+v+\frac{3}{2}\right)} \left(\frac{x}{2}\right)^{2k} \tag{3.3}$$

There is a recurrence relation between the Struve functions not unlike that given above for the Bessel functions. We have [3, p. 496]

$$H_{v+1}(x) = \frac{2v}{x} H_v(x) - H_{v-1}(x) + \frac{1}{\sqrt{\pi}\Gamma\left(v+\frac{3}{2}\right)} \left(\frac{x}{2}\right)^v \tag{3.4}$$

In particular, with $v = 0$ and since $\Gamma(3/2) = \sqrt{\pi}/2$,

$$H_1(x) = \frac{2}{\pi} - H_{-1}(x) \tag{3.5}$$

and, with $v = 1$ and since $\Gamma(5/2) = 3\sqrt{\pi}/4$,

$$H_2(x) = \frac{2x}{3\pi} + \frac{2}{x} H_1(x) - H_0(x) \tag{3.6}$$

There is also a relationship between derivatives similar to that for the Bessel functions. From [3, p. 496],

$$H_{v-1}(x) - H_{\nu+1}(x) = 2\frac{d}{dx} H_\nu(x) - \frac{1}{\sqrt{\pi}\Gamma\left(v+\frac{3}{2}\right)} \left(\frac{x}{2}\right)^v \tag{3.7}$$

For $\nu = 0$, we have

$$\frac{d}{dx} H_0(x) = \frac{1}{\pi} + \tfrac{1}{2} H_{-1}(x) - \tfrac{1}{2} H_1(x) \tag{3.8}$$

which by equation (3.5) reduces to

$$\frac{d}{dx} H_0(x) = \frac{2}{\pi} - H_1(x) \tag{3.9}$$

Similarly, for $\nu = 1$,

$$\frac{d}{dx} H_1(x) = \frac{x}{3\pi} + \tfrac{1}{2} H_0(x) - \tfrac{1}{2} H_2(x) \tag{3.10}$$

which reduces, by equation (3.6), to

$$\frac{\mathrm{d}}{\mathrm{d}x}H_1(x) = H_0(x) - \frac{1}{x}H_1(x). \tag{3.11}$$

The above material enables the supply of simple proofs to the following theorems.

Theorem 1. The following identity holds:

$$\int \mathcal{J}_0(x)\,\mathrm{d}x = x\mathcal{J}_0(x) + \left\{\frac{\pi}{2}x\mathcal{J}_1(x)H_0(x) - \frac{\pi}{2}x\mathcal{J}_0(x)H_1(x)\right\} \tag{3.12}$$

Proof. The derivative of the right-hand side is

$$\mathcal{J}_0(x) + x\frac{\mathrm{d}}{\mathrm{d}x}\mathcal{J}_0(x) + \frac{\pi}{2}\mathcal{J}_1(x)H_0(x) + \frac{\pi}{2}x\left(\frac{\mathrm{d}}{\mathrm{d}x}\mathcal{J}_1(x)\right)H_0(x) + \frac{\pi}{2}x\mathcal{J}_1(x)\left(\frac{\mathrm{d}}{\mathrm{d}x}H_0(x)\right)$$
$$-\frac{\pi}{2}\mathcal{J}_0(x)H_1(x) - \frac{\pi}{2}x\left(\frac{\mathrm{d}}{\mathrm{d}x}\mathcal{J}_0(x)\right)H_1(x) - \frac{\pi}{2}x\mathcal{J}_0(x)\left(\frac{\mathrm{d}}{\mathrm{d}x}H_1(x)\right) \tag{3.13}$$

and by equations (3.9), (3.11), (2.9) and (2.7) this becomes

$$\mathcal{J}_0(x) - x\mathcal{J}_1(x) + \frac{\pi}{2}\mathcal{J}_1(x)H_0(x) + \frac{\pi}{2}x(\mathcal{J}_0(x) - \frac{1}{x}\mathcal{J}_1(x))H_0(x)$$
$$+\frac{\pi}{2}x\mathcal{J}_1(x)\left(\frac{2}{\pi} - H_1(x)\right) - \frac{\pi}{2}\mathcal{J}_0(x)H_1(x) + \frac{\pi}{2}x\mathcal{J}_1(x)H_1(x)$$
$$-\frac{\pi}{2}x\mathcal{J}_0(x)(H_0(x) - \frac{1}{x}H_1(x)) \tag{3.14}$$

which in turn reduces to $\mathcal{J}_0(x)$ and the proof is complete. Note that in this simplification, we have shown:

Corollary 1. The following identity holds:

$$\frac{\mathrm{d}}{\mathrm{d}x}\left\{\frac{\pi}{2}x\mathcal{J}_1(x)H_0(x) - \frac{\pi}{2}x\mathcal{J}_0(x)H_1(x)\right\} = x\mathcal{J}_1(x) \tag{3.15}$$

Theorem 2. The following identity holds:

$$\int x^2\mathcal{J}_0(x)\,\mathrm{d}x = x^2\mathcal{J}_1(x) - \left\{\frac{\pi}{2}x\mathcal{J}_1(x)H_0(x) - \frac{\pi}{2}x\mathcal{J}_0(x)H_1(x)\right\} \tag{3.16}$$

Proof. The derivative of the first term of the right-hand side is

$$x\mathcal{J}_1(x) + x^2\mathcal{J}_0(x) \tag{3.17}$$

as can easily be verified by using equations (2.6) and (2.10). The derivative of the two terms within the curly brackets of the right-hand side is given in equation (3.15) and thus the result follows.

4. Fourier–Bessel series

In a beginning partial differential equations course, students are introduced to Sturm–Liouville theory and the notions of eigenfunction and eigenvalue. When solving the circular drumhead problem, typical in such a course, Bessel's equation of order 0 arises and it turns out that the eigenvalues are the positive roots λ_n of the

Bessel function $\mathcal{J}_0(x)$ and the eigenfunctions are $\phi_n(x) = \mathcal{J}_0(\lambda_n x)$. From Sturm–Liouville theory, it follows that the functions $\{\phi_n\}$ are orthogonal with respect to the weight function $w(x) = x$, and thus we have, for positive integers $n \neq m$,

$$\int_0^1 x\mathcal{J}_0(\lambda_n x)\mathcal{J}_0(\lambda_m x)\,\mathrm{d}x = 0 \tag{4.1}$$

This family of eigenfunctions now can be used to form the basis functions for the Fourier–Bessel series (of order 0). Given a piecewise very smooth function $f(x)$ (the second derivative of f is piecewise continuous) defined over the closed interval $[0, 1]$, the Fourier–Bessel series for f is the series

$$\sum_{n=1}^{\infty} c_n \mathcal{J}_0(\lambda_n x) \tag{4.2}$$

where the coefficients c_n are calculated from the formula

$$c_n = \frac{\displaystyle\int_0^1 xf(x)\mathcal{J}_0(\lambda_n x)\,\mathrm{d}x}{\displaystyle\int_0^1 x\mathcal{J}_0(\lambda_n x)^2\,\mathrm{d}x} \tag{4.3}$$

To simplify this we need

Theorem 3. The following identity holds:

$$\int u\mathcal{J}_0(u)^2\,\mathrm{d}u = \tfrac{1}{2}\Big\{u^2\mathcal{J}_0(u)^2 + u^2\mathcal{J}_1(u)^2\Big\} \tag{4.4}$$

Proof. The derivative of the right-hand side is easily computed using the formulas developed in section 2.

It follows directly from Theorem 3 that

$$\int_0^1 x\mathcal{J}_0(\lambda_n x)^2\,\mathrm{d}x = \tfrac{1}{2}\mathcal{J}_1(\lambda_n)^2 \tag{4.5}$$

Thus we can set

$$c_n = \frac{2}{\mathcal{J}_1(\lambda_n)^2}\int_0^1 xf(x)\mathcal{J}_0(\lambda_n x)\,\mathrm{d}x \tag{4.6}$$

Just as for the theory of Fourier series, the Fourier–Bessel series of $f(x)$ converges to $f(x)$ whenever the series itself is uniformly convergent, which is the case, for example, when $f(x)$ has a continuous second derivative and $f(1) = 0$. Note that this last requirement is necessary since at $x = 1$, every function $\mathcal{J}_0(\lambda_n x)$ is 0. If the second derivative of $f(x)$ is merely piecewise continuous, then the Fourier–Bessel series is uniformly convergent over any subinterval not containing a point of discontinuity. If the interval contains a jump discontinuity point, then the convergence is pointwise and converges to the average of the left- and right-hand limits, just as is the case for Fourier series for a piecewise continuous function. For a readable exposition on the elementary facts concerning orthogonal functions and Fourier–Bessel series we refer the reader to [5].

Because of the importance of these series, there has been a great deal of programming effort put into calculating the zeros of the function $\mathcal{J}_0(x)$. For example, in *Mathematica*, there is a command **BesselJZeros[ν, k]** which will compute the first k zeros of $\mathcal{J}_\nu(x)$. For more details, see [6].

5. The Gibbs' phenomenon for Fourier series

Recall that for a periodic function $f(x)$, say of period 2π, with $f(x)$ piecewise continuous and piecewise smooth, then there is an effect that occurs near each jump discontinuity of $f(x)$ called the Gibbs' effect when using truncated Fourier series to approximate $f(x)$. This is most often illustrated with the step function

$$f(x) = \begin{cases} -1 & -\pi < x < 0 \\ 0 & x = -\pi, 0, \pi \\ 1 & 0 < x < \pi \end{cases} \tag{5.1}$$

which is extended periodically. Figure 3 plots $f(x)$ and the sum of the first ten terms and the sum of the first 100 terms of the Fourier series for $f(x)$. One can

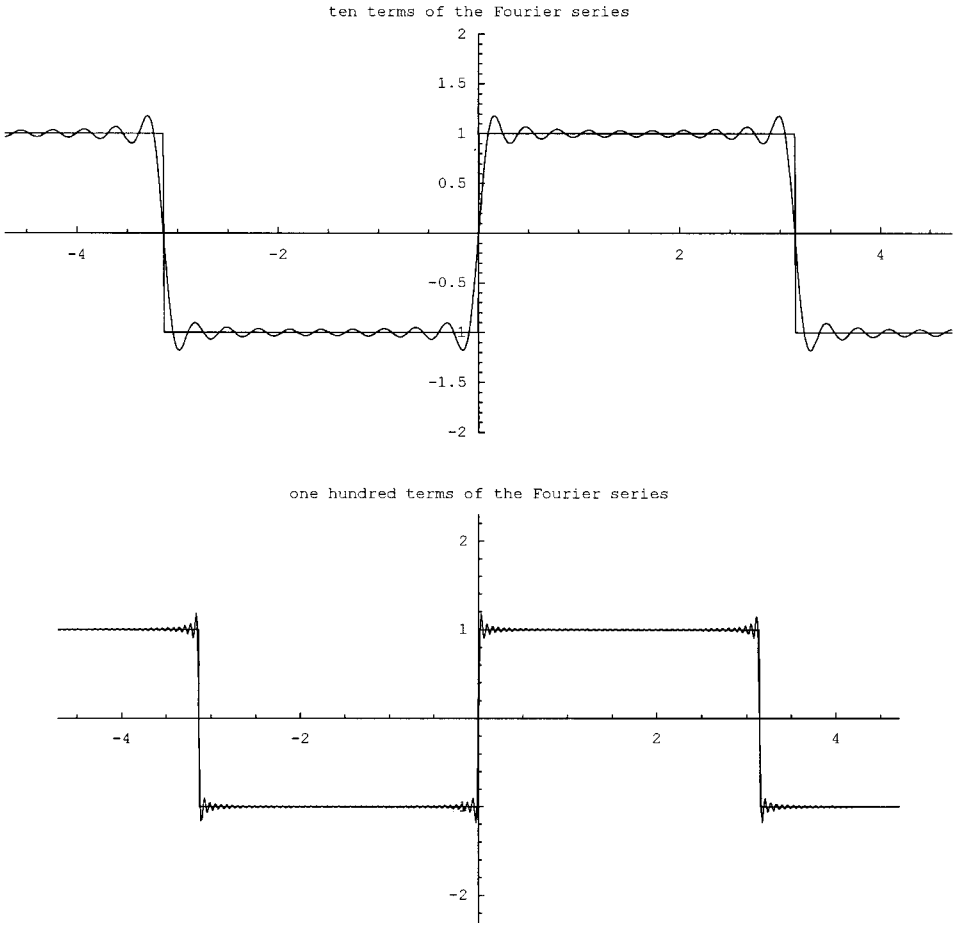

Figure 3. The step function f and partial sums of its Fourier series.

clearly see that although the Fourier series for $f(x)$ converges pointwise to $f(x)$ at each value of x, the 'under- and over-shoots' just to the left and right of the jump discontinuities do not disappear as n tends to infinity, but rather tend to a well defined-limit, which can be shown to be

$$\frac{2}{\pi}\int_0^{\pi}\frac{\sin x}{x}\,\mathrm{d}x - 1 \approx 0.178\,979\,744 \tag{5.2}$$

This phenomenon occurs not just for step functions, but whenever $f(x)$ has a jump discontinuity, and has been the subject of the two recent articles [1] and [2] in this journal.

6. The Gibbs' phenomenon for Fourier–Bessel series

To expand a function in a Fourier–Bessel series, it is assumed that the function has domain $[0, 1]$ and the description

$$f(x) = \sum_{n=1}^{\infty} c_n \mathcal{J}_0(\lambda_n x) \tag{6.1}$$

is used, where, for simplicity, it is assumed that $f(1) = 0$, f has a piecewise continuous second derivative, and at any point of discontinuity x_0,

$$f(x_0) = \tfrac{1}{2}\{\lim_{x\to x_0^-} f(x) + \lim_{x\to x_0^+} f(x)\} \tag{6.2}$$

so that the Fourier–Bessel series for $f(x)$ converges pointwise to $f(x)$. The formula for the coefficients c_n is given above in equation (4.6).

6.1. *A simple step function*

We first consider the simple example of a step function

$$g(x) = \begin{cases} 1 & 0 \le x < \frac{1}{2} \\ 1/2 & x = 1/2 \\ 0 & \frac{1}{2} < x \le 1 \end{cases} \tag{6.3}$$

To investigate the Fourier–Bessel series approximations of $g(x)$, set

$$\Phi_n(x) = \sum_{k=1}^{n} c_k \mathcal{J}_0(\lambda_k x) \tag{6.4}$$

and plot $g(x)$ and Φ_{10}, and Φ_{100} (figure 4).

A Gibbs' phenomenon can be seen quite clearly in these figures.

For this step function $g(x)$, the Fourier–Bessel coefficients c_n are easy to calculate. First note that from equation (2.12), letting $u = \lambda_n x$,

$$\begin{aligned}\int x\mathcal{J}_0(\lambda_n x)\,\mathrm{d}x &= \frac{1}{\lambda_n^2}\int u\mathcal{J}_0(u)\,\mathrm{d}u \\ &= \frac{1}{\lambda_n} x\mathcal{J}_1(\lambda_n x)\end{aligned} \tag{6.5}$$

and thus

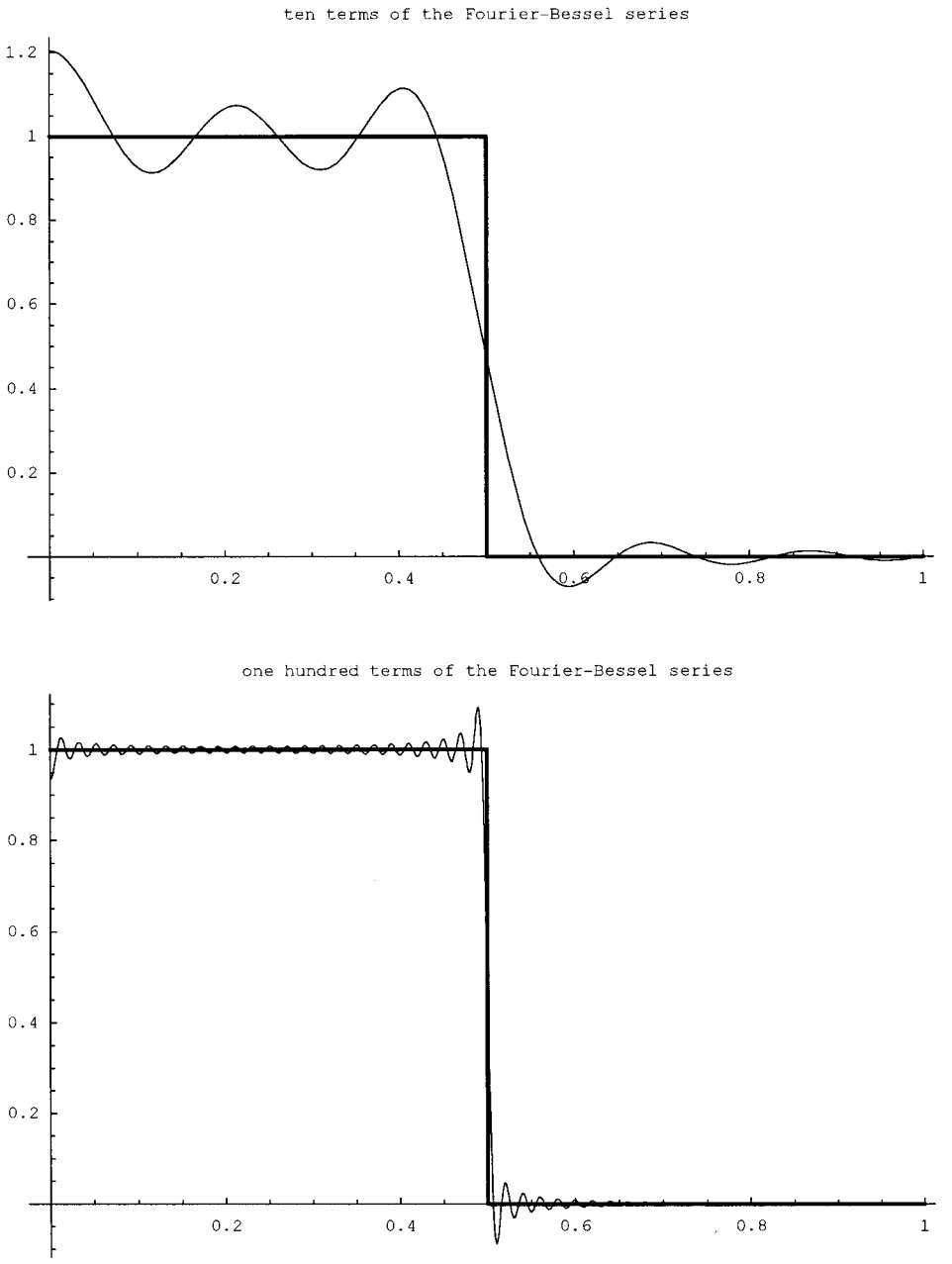

Figure 4. The function g and partial sums of its Fourier–Bessel series.

$$\int_0^1 xg(x)\mathcal{J}_0(\lambda_n x)\,\mathrm{d}x = \int_0^{1/2} x\mathcal{J}_0(\lambda_n x)\,\mathrm{d}x$$
$$= \frac{1}{2\lambda_n}\mathcal{J}_1\left(\frac{\lambda_n}{2}\right) \tag{6.6}$$

From equation (4.6), it follows that

$$c_n = \frac{1}{\lambda_n}\frac{\mathcal{J}_1(\lambda_n/2)}{\mathcal{J}_1(\lambda_n)^2} \tag{6.7}$$

Thus the nth partial sum of the Fourier–Bessel series for $g(x)$ is given by

$$\Phi_n(x) = \sum_{k=1}^{n} \frac{\mathcal{J}_1(\lambda_k/2)}{\lambda_k(\mathcal{J}_1(\lambda_k))^2}\mathcal{J}_0(\lambda_k x) \tag{6.8}$$

We will investigate the over- and under-shoot just to the right and left of $x = 1/2$. The value of x to the immediate left of $1/2$ for which $\Phi_n(x)$ is a maximum is denoted xL_n, and the value of x just to the immediate right of $1/2$ for which $\Phi_n(x)$ is a minimum is denoted xR_n. This is illustrated for $n = 10$ in figure 5.

The Fourier–Bessel series representation is a slowly converging series. The values of xL_n and xR_n have to be computed using Newton's method or the secant method or some other numerical routine. It turns out that, generally speaking, xL_n and xR_n are very close to being the rationals $(n-2)/2n$ and $(n+2)/2n$. In table 1 these values are computed for representative values of n. The values have been rounded to six decimal places.

Table 2 computes the over-shoot $\Phi_n(xL_n) - 1$, the under-shoot $0 - \Phi_n(xR_n)$, and their sum.

Table 2 shows that as n increases, the over-shoot decreases and the undershoot increases, and these values appear to be converging to the same number. The sum of the two appears to be decreasing and converging to the number 0.178 980. It is

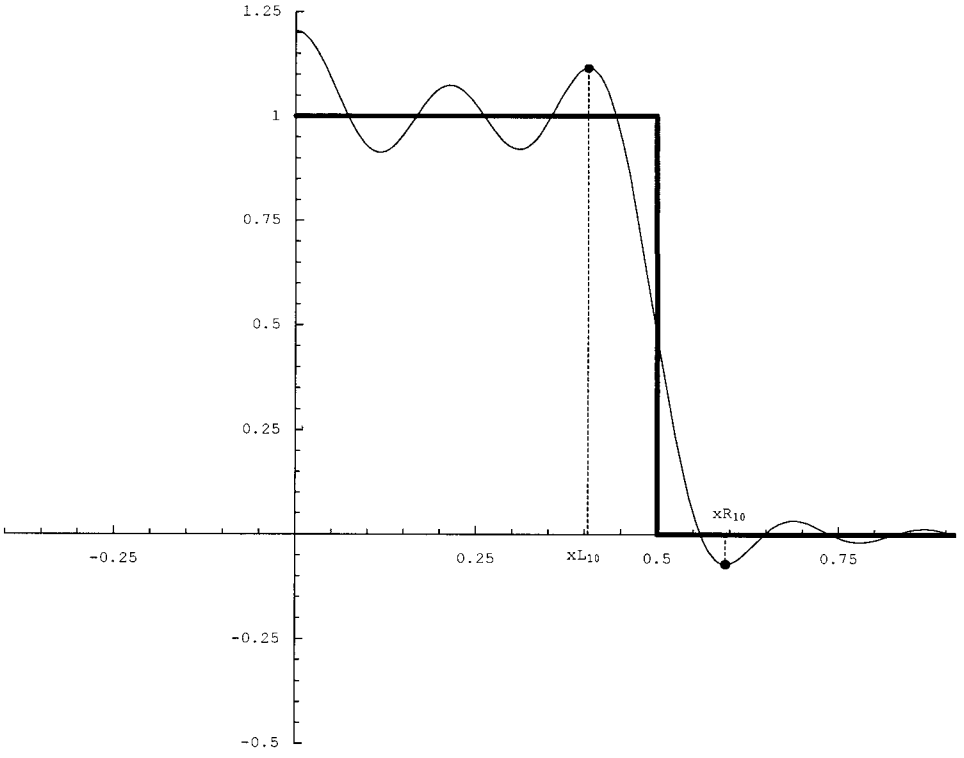

Figure 5. Ten terms of the Fourier–Bessel series for g showing xL_{10} and xR_{10}.

n	xL_n	$(n-2)/2n$	Difference	xR_n	$(n+2)/2n$	Difference
10	0.405 094	2/5	$-0.005\,094$	0.594 186	3/5	0.005 814
50	0.480 233	12/25	$-0.000\,233$	0.519 761	13/25	0.000 239
100	0.490 059	49/100	$-0.000\,059$	0.509 940	51/100	0.000 060
500	0.498 002	249/500	-2.4×10^{-6}	0.501 998	251/500	2.4×10^{-6}
1000	0.499 001	499/1000	-6.0×10^{-7}	0.500 999	501/1000	6.0×10^{-7}
5000	0.499 800	2499/5000	-2.4×10^{-8}	0.500 200	2501/5000	2.4×10^{-8}

Table 1. Values of xL_n, xR_n, $(n-2)/2$ and $(n+2)/2n$.

n	Over-shoot	Under-shoot	Sum
10	0.114 482	0.071 318	0.185 800
50	0.093 903	0.085 365	0.179 269
100	0.091 662	0.087 390	0.179 053
500	0.089 919	0.089 064	0.178 983
1 000	0.089 704	0.089 276	0.178 980
5 000	0.089 533	0.089 447	0.178 980
10 000	0.089 511	0.089 468	0.178 980

Table 2. Over-shoot, under-shoot and their sum.

interesting to observe that this number is exactly the Gibbs' constant rounded to six decimal places:

$$\frac{2}{\pi}\int_0^{\pi}\frac{\sin x}{x}\,\mathrm{d}x - 1 \approx 0.178\,979\,744 \tag{6.9}$$

One could carry on computing with larger values of n, given the stamina. There is a trade-off between calculations, accuracy, and length of time for the computations to be completed. In fact, for $n = 50\,000$, and computing[2] with a working precision of 21, so that *Mathematica* attempts to compute at each step with 11 digit accuracy, the difference between the Gibbs' constant and the sum of the over-shoot and under-shoot is less than 3×10^{-10}.

Finally, observe that the Gibbs' constant for Fourier series computations is

$$\frac{2c}{\pi}\int_0^{\pi}\frac{\sin x}{x}\,\mathrm{d}x - c \tag{6.10}$$

where the constant c is one-half the value of the jump. Thus for the function $g(x)$, the value of c is exactly 1/2 and so the Gibbs' constant for this function is 0.089 489 872, and it is believable that the over- and under-shoots are converging to this value.

Conjecture. For any piecewise very smooth function having a jump discontinuity of height $2c$, the over- and under-shoots converge to the value

$$\frac{2c}{\pi}\int_0^{\pi}\frac{\sin x}{x}\,\mathrm{d}x - c \tag{6.11}$$

[2] These computations were performed on a PC running dual 1 GHz Pentium III processors and having 2 GB RAM.

6.2. *A linear example*

It is very risky to make a conjecture on the basis of one numerical investigation. Therefore, consider a different example. Consider the function $h(x)$ defined by

$$h(x) = \begin{cases} 2x & 0 \leq x < \frac{1}{2} \\ \frac{1}{2} & x = \frac{1}{2} \\ 0 & \frac{1}{2} < x \leq 1 \end{cases} \tag{6.12}$$

This function too has a jump discontinuity of value 1 and if our conjecture is true, then one would expect to see a similar pattern of over- and under-shoots converging as above.

The Fourier–Bessel series for $h(x)$ is

$$\Psi(x) = \sum_{n=1}^{\infty} c_n \mathcal{J}_0(\lambda_n x) \tag{6.13}$$

with coefficients

$$c_n = \frac{1}{\lambda_n (\mathcal{J}_1(\lambda_n))^2} \left\{ \mathcal{J}_1(\lambda_n/2) - \frac{\pi}{\lambda_n} (\mathcal{J}_1(\lambda_n/2) H_0(\lambda_n/2) - \mathcal{J}_0(\lambda_n/2) H_1(\lambda_n/2)) \right\} \tag{6.14}$$

the nth partial sum is denoted by $\Psi_n(x)$. For this function $h(x)$, the calculation of the coefficients c_n follow easily from Theorem 2 and equation (4.6). Plots of this function and Fourier–Bessel series approximations to it are shown in figure 6.

Again, it is seen that the Fourier–Bessel series representation is slowly converging. The values of xL_n and xR_n, determined by the derivatives of the partial sums of the Fourier–Bessel series, are computed using the *Mathematica* command **FindRoot** which employs Newton's method. Newton's method requires an initial value which we choose to be $(n-2)/2n$ for xL_n and $(n+2)/2n$ for xR_n. Table 3 shows these values for representative values of n. The values have been rounded to six decimal places.

Table 4 shows computations of the 'over-shoot' $\Psi_n(xL_n) - 2xL_n$, the under-shoot $0 - \Psi_n(xR_n)$, and their sum.

The computational time to generate these numbers is considerably more than that for the first example. This is due to the much larger number of functional evaluations needed to calculate the coefficients c_n and to the fact that the evaluations of the Struve functions take some time to converge.

It certainly appears from the data that as n increases, the over-shoot is decreasing and the under-shoots are increasing, converging to

$$0.089\,489\,872 \approx \frac{1}{\pi} \int_0^{\pi} \frac{\sin x}{x} \, \mathrm{d}x - \tfrac{1}{2} \tag{6.15}$$

supporting our conjecture above.

6.3. *A quadratic example*

Now consider a more complex example. Consider the function $k(x)$ defined by

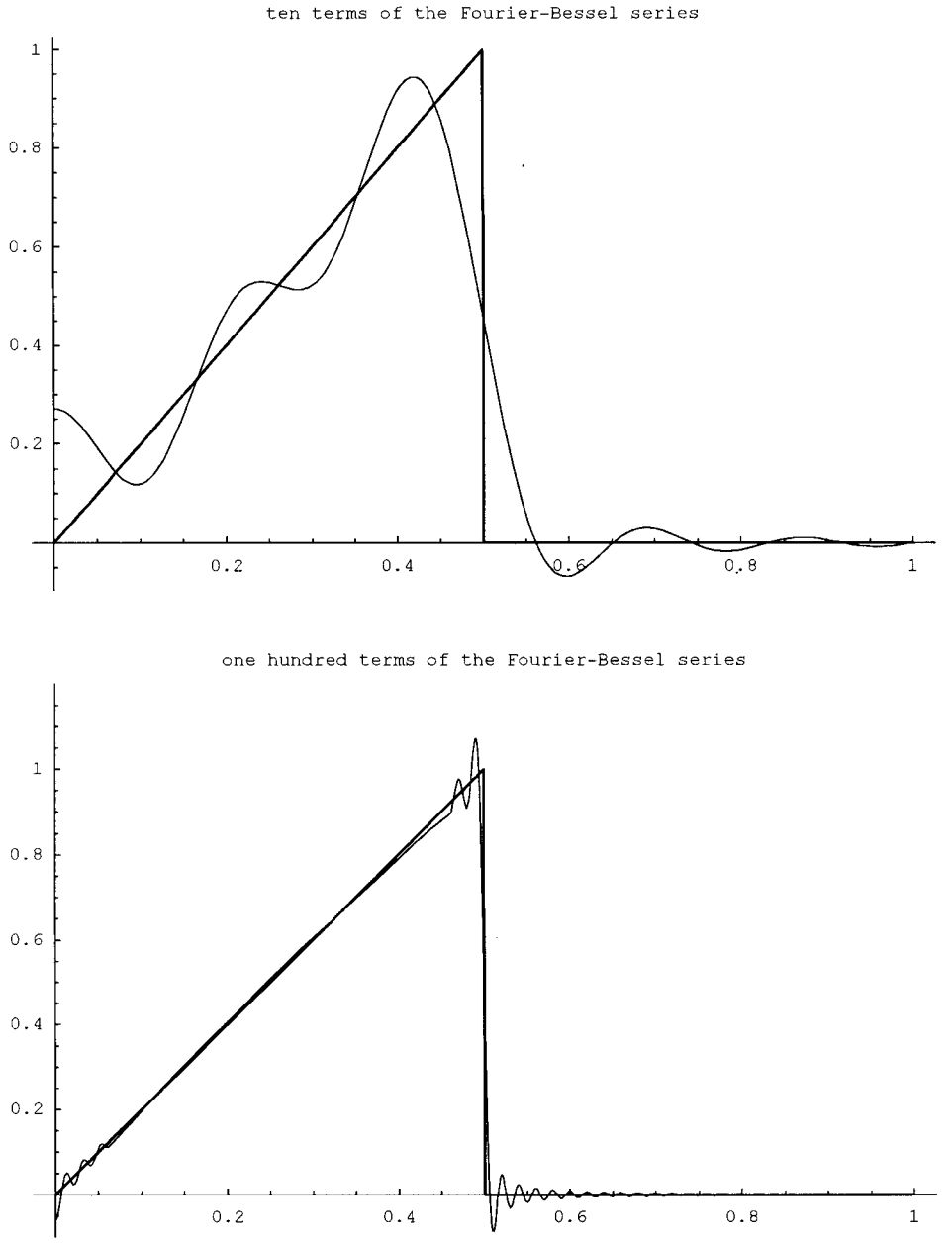

Figure 6. The function h and partial sums of its Fourier–Bessel series.

$$k(x) = \begin{cases} 4x^2 & 0 \le x < \frac{1}{2} \\ 0 & x = \frac{1}{2} \\ 2x - 2 & \frac{1}{2} < x \le 0 \end{cases} \tag{6.16}$$

This function has a jump discontinuity of value 2 and we expect to see over- and under-shoots converging to twice that which was observed previously (figure 7).

n	xL_n	$(n-2)/2n$	Difference	xR_n	$(n+2)/2n$	Difference
10	0.419 020	2/5	− 0.019 020	0.596 427	3/5	0.003 573
50	0.481 018	12/25	− 0.001 018	0.519 836	13/25	0.000 165
100	0.490 266	49/100	− 0.000 266	0.509 958	51/100	0.000 042
200	0.495 068	249/500	− 0.000 068	0.504 990	251/500	0.000 010

Table 3. Results for a linear example.

n	Over-shoot	Under-shoot	Sum
10	0.105 947	0.067 658	0.173 605
50	0.093 728	0.084 842	0.178 570
100	0.091 724	0.087 144	0.178 868
200	0.090 641	0.088 310	0.178 950

Table 4. Over/under-shoot and sum for linear examples.

The Fourier–Bessel series for $k(x)$ is

$$\Omega(x) = \sum_{n=1}^{\infty} c_n \mathcal{J}_0(\lambda_n x) \tag{6.17}$$

with coefficients

$$\begin{aligned} c_n = \frac{2}{\mathcal{J}_1(\lambda_n)^2} \Bigg\{ & \frac{2}{\lambda_n^2}\mathcal{J}_0(\lambda_n/2) - \frac{8}{\lambda_n^3}\mathcal{J}_1(\lambda_n/2) + \frac{1}{\lambda_n}\mathcal{J}_1(\lambda_n/2) \\ & + \frac{\pi}{2\lambda_n^2}(\mathcal{J}_1(\lambda_n/2)H_0(\lambda_n/2) - \mathcal{J}_0(\lambda_n/2)H_1(\lambda_n/2)) \\ & - \frac{\pi}{\lambda_n^2}(\mathcal{J}_1(\lambda_n)H_0(\lambda_n)) \Bigg\} \end{aligned} \tag{6.18}$$

The nth partial sum is denoted by $\Omega_n(x)$. The approximation $\Omega_{300}(x)$ is shown in figure 7; note that this Fourier–Bessel series is also apparently slow to converge.

In order to verify equation (6.18), one needs to compute

$$\int_0^{1/2} 4x^3 \mathcal{J}_0(\lambda_n x)\,\mathrm{d}x + \int_{1/2}^{1} (2x^2 - 2x)\mathcal{J}_0(\lambda_n x)\,\mathrm{d}x \tag{6.19}$$

To do so requires:

Theorem 4. The following identity holds:

$$\begin{aligned} \int x^3 \mathcal{J}_0(x)\,\mathrm{d}x &= 2x^2\mathcal{J}_2(x) - x^3\mathcal{J}_3(\lambda x) \\ &= 2x^2\mathcal{J}_0(x) + (x^3 - 4x)\mathcal{J}_1(x) \end{aligned} \tag{6.20}$$

Proof. The proof of this is straightforward; differentiate the right-hand side and use equations (2.9), (2.10), and (2.8).

The verification of equation (6.18) now follows from equations (4.6), (2.12), (3.16), and (6.20).

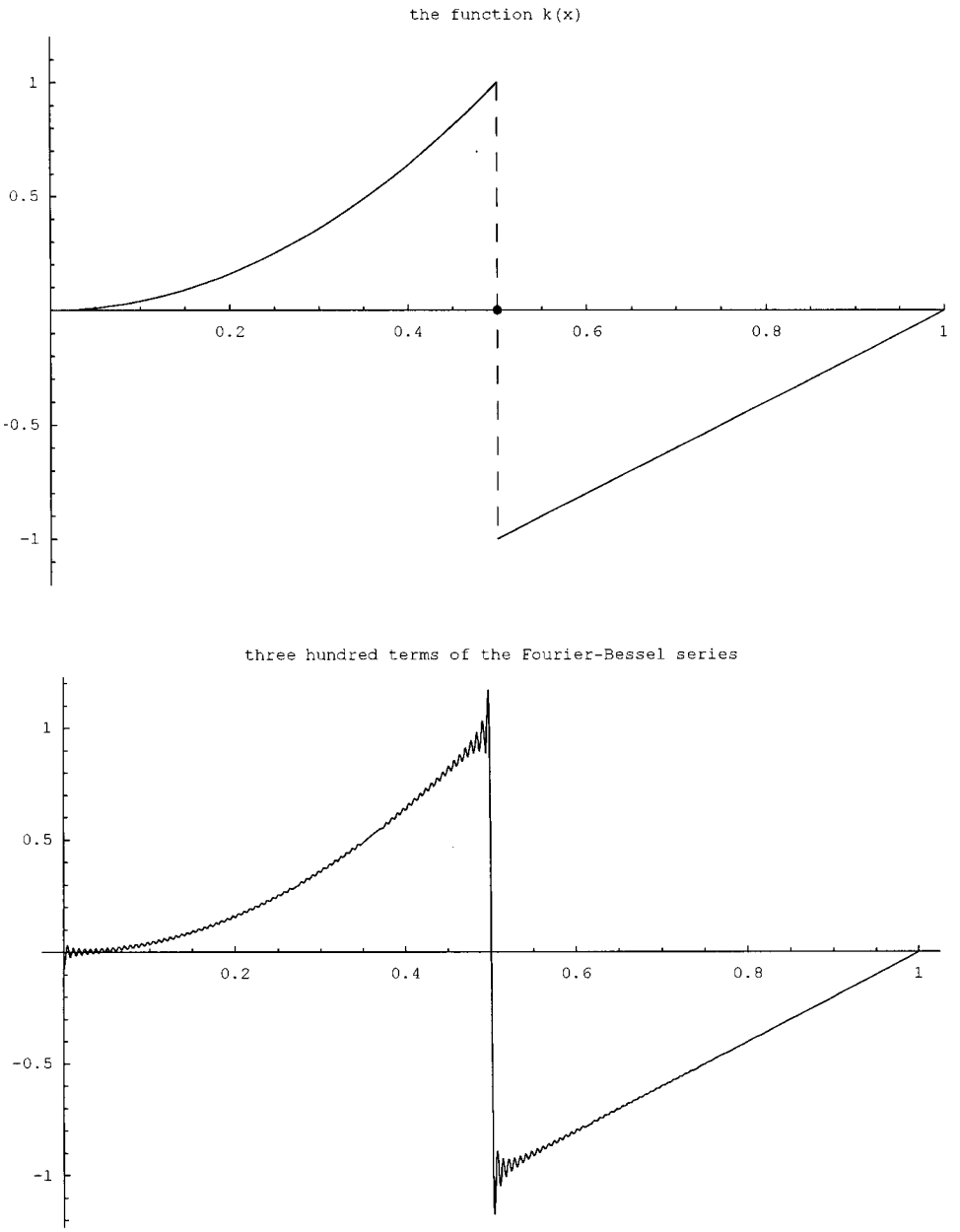

Figure 7. The function k and the first 300 terms of the Fourier–Bessel series.

Table 5 lists the over-shoot $\Omega_n(xL_n) - 2Lx_n$ and the under-shoot $0 - \Omega_n(xR_n)$.

Based on this numerical evidence, our conjecture again appears to be valid. It is possible to compute values for n larger than 400, but at an unreasonable time cost. To compute c_n for $n = 500$ took well over 24 hours on a 500 MHz PC.

6.4. *Improving the speed of the calculations*

It appears that the slowdown is taking place with the evaluation of the Struve functions. Attempting a simple plot of $H_0(x)$ for x between 200 and 1000 takes too

n	Over-shoot	Under-shoot
100	0.183 18	0.174 47
200	0.181 12	0.176 76
300	0.180 41	0.177 51
400	0.180 05	0.177 89

Table 5. Results for quadratic examples.

much time to be 'user friendly'. This leads us to seek asymptotic approximations of the Struve functions for large values of x. Fortunately these are well known and given in [3] ; for large values of x, $H_0(x)$ and $H_1(x)$ are very nearly equal to $Y_0(x)$ and $Y_1(x)$ respectively, as we see from the following formulas.

$$H_0(x) \approx Y_0(x) + \frac{2}{\pi}\left\{\frac{1}{x} - \frac{1}{x^3} + \frac{1^2 \times 3^2}{x^5} - \frac{1^2 \times 3^2 \times 5^2}{x^7} + \cdots\right\}$$

$$H_1(x) \approx Y_1(x) + \frac{2}{\pi}\left\{1 + \frac{1}{x^2} - \frac{1^2 \times 3}{x^4} + \frac{1^2 \times 3^2 \times 5}{x^6} - \frac{1^2 \times 3^2 \times 5^2 \times 7}{x^8} + \cdots\right\}$$

If we investigate (by plotting) the difference between $H_0(x)$ and the approximation

$$Y_0(x) + \frac{2}{\pi}\left\{\frac{1}{x} - \frac{1}{x^3} + \frac{1^2 \times 3^2}{x^5} - \frac{1^2 \times 3^2 \times 5^2}{x^7}\right\}$$

then it is seen that as x increases, the difference or error in absolute value decreases. For x between 50 and 60, for example, the error is less than 5×10^{-10}, and for x between 60 and 70, the error is less than 1×10^{-12}. For $x \geq 50$, the approximation yields nine decimal place accuracy. The approximation

$$Y_1(x) + \frac{2}{\pi}\left\{1 + \frac{1}{x^2} - \frac{1^2 \times 3}{x^4} + \frac{1^2 \times 3^2 \times 5}{x^6} - \frac{1^2 \times 3^2 \times 5^2 \times 7}{x^8}\right\}$$

to $H_1(x)$, for $x \geq 50$, the error is bounded by 4×10^{-11}, yielding 10 decimal place accuracy. Moreover, plotting the approximations over intervals for large x is virtually instantaneous, which suggests that these approximations will alleviate the computation time problem.

Rather arbitrarily, it was decided to start using the approximations for the Struve functions when the argument is 50 or more. Since we wish to evaluate the Struve functions at $\lambda_n/2$, we need n to be 33 or larger, since λ_n is less than 100 for $n < 33$, and $\lambda_{33} = 102.8884$.

Using this approach, it was straightforward to calculate the overshoot and under-shoot for $n \geq 500$ (table 6).

Comparing with the calculations above, we see that both the overshoots and undershoots are increasing. However, there are other potential numerical problems. The derivative of the Fourier–Bessel series approximation is highly oscillatory, and therefore the Newton's method routine **FindRoot** used to calculate xL_n and xR_n is very sensitive to the starting point. A small difference in starting points gives quite different values, and consequently different over-shoots or undershoots. Starting values $(n-2)/2n$ and $(n+2)/2n$ work very well.

n	Over-shoot	Under-shoot
500	0.179 87	0.178 08
600	0.179 72	0.178 23
700	0.179 62	0.178 33
1000	0.179 43	0.178 53
1500	0.179 28	0.178 68
2000	0.179 20	0.178 75

Table 6. Results for improved speed version.

n	xL_n	$(n-2)/2n$	Difference	xR_n	$(n+2)/2n$	Difference
200	0.495 068	198/400	0.000 068	0.504 989	202/400	0.000 011
1000	0.499 003	499/1000	−0.000 003	0.501 000	501/1000	0.000 000
2000	0.499 501	1998/4000	1×10^{-6}	0.500 500	2002/4000	0.000 000

Table 7. Results for the linear example and improved speed version.

n	Over-shoot	Under-shoot	Sum
200	0.090 640 9	0.088 309 5	0.178 950 4
1000	0.089 725 9	0.089 252 6	0.178 978 5
2000	0.089 608 3	0.089 371 2	0.178 979 5

Table 8. Over/under-shoot and sum for linear example: improved speed.

6.5. *The linear example revisited*

Returning to the linear example $h(x)$ above, with the partial sum $\Psi_n(x)$ of the Fourier–Bessel series, we use the values c_n calculated by equation (6.14) for $n \leq 12$, and for $n > 12$, we replace the Struve functions by their asymptotic expansions in equation (6.14). This leads to the calculations (rounded to six decimals) shown in table 7.

Table 8 shows the over-shoot $\psi_n(xL_n) - 2xL_n$, the under-shoot $0 - \Psi_n(xR_n)$, and their sum, computed to seven decimal places.

This reinforces the assertion made at the end of the discussion above for this example, that the conjecture appears to be true.

7. Conclusions

While these numerical investigations are not absolutely conclusive, it is believed that the Gibbs' constant for a jump discontinuity for Fourier–Bessel series expansions is the same as that for Fourier series. This raises the question, of course, why should this be true? Is it coincidence, or is there a fundamental principle involved here? Further investigations are suggested.

- Provide a theoretical proof that the Gibbs' constants are the same. Is this constant a result of the convergence in the $\mathcal{L}_2$-norm?

- Fourier–Bessel series of the first kind of order ν are defined in an analogous way as we have done for the Bessel functions of order 0 and these series have similar convergence properties. We expect a Gibbs' phenomenon for these series as well. Is the Gibbs' constant the same?
- Legendre polynomials are orthogonal and can be used to produce Fourier–Legendre series for functions defined over $[-1, 1]$. Is there a Gibbs' phenomenon at a jump discontinuity and if so, is the Gibbs' constant the same?
- There are other collections of orthogonal polynomials—Chebyshev, Hermite, Jacobi, Laguerre—each collection yielding a complete orthogonal system over an appropriate interval, which can produce series. And of course there are general Sturm–Liouville series. What is the situation for these series with respect to a Gibbs' phenomenon?

It is believed that numerical investigations, such as those outlined above, can be effective in illustrating the need for theoretical work and that the one goes hand-in-hand with the other. For example, the description of the Fourier–Bessel series coefficients given by Sturm–Liouville theory as integral formulas are not necessarily 'user-friendly' and further theoretical work permits the discovery of 'computational-friendly' forms. Asymptotic formulas are not fully appreciated until one has waited several hours for seemingly simple computations to be performed. And interactive graphical analysis provided by the software used in conjunction with the theory and numerics makes the whole process more understandable and, we would aver, more enjoyable. The Gibbs' phenomenon provides a beautiful visual problem and a framework for understanding much of the general theory in beginning analysis.

References

[1] Fay, T. H., and Kloppers, P. H., 2001, *Int. J. Math. Educ. Sci. Technol.*, **32,** 73–89.
[2] Fay, T. H., and Schulz, K. G., 2001, *Int. J. Math. Educ. Sci. Technol.*, **32,** 863–872.
[3] Abramowitz, M., and Stegun, I. A., 1968, *Handbook of Mathematical Functions* (National Bureau of Standards, US Dept. of Commerce).
[4] Thompson, W. J., 1997, *Atlas for Computing Mathematical Functions* (New York: John Wiley & Sons).
[5] Kaplan, W., 1952, *Advanced Calculus* (Reading, MA: Addison-Wesley).
[6] Wolfram, S., 1996, *The Mathematica Book*, 3rd edn (New York: Wolfram Media/ Cambridge University Press).